Sand2005-4361c

Simulation of Mixed Oxide (MOX) Versus Low Enrichment Uranium (LEU) Fuel Severe Accident Response Using MELCOR

S.G. Ashbaugh[1], K.C. Wagner[2] and R.O. Gauntt[1]

[1]*Sandia National Laboratories, PO Box 5800, Albuquerque, NM 87185-0748, sgashba@sandia.gov*
[2]*dycoda LLC, 267 Los Lentes Road NE, Los Lunas, NM 87031, kcw@dycoda.com*

Abstract – The U.S. Department of Energy (DOE) plans to dispose of up to 33 tons of excess weapons-grade plutonium (WG-Pu) by irradiating it in the form of mixed-oxide (MOX) fuel in four U.S. commercial pressurized-water reactors (PWRs). The U.S. Nuclear Regulatory Commission (NRC) has initiated a study to evaluate the impact of using MOX fuels at these reactors. Responsible studies of operational risk must begin by estimating the potential radiological release to the environment (or source term) that could be postulated by an accident involving substantial meltdown of the reactor fuel. This paper describes the results of a study to develop representative source terms for such accidents using mechanistic MELCOR severe accident simulations. These simulations compare calculated radiological source terms for postulated accidents involving present-day low-enriched uranium (LEU) fuels with those that involve MOX fuels.

I. INTRODUCTION

As part of a U.S. NRC research program to evaluate the impact of using MOX fuel in commercial nuclear power plants, a study was undertaken to evaluate the usage of MOX fuel during postulated severe accidents. Two PWRs with ice condenser containments are currently planning to burn MOX fuel in support of a U.S. DOE initiative to dispose of WG-Pu. The plant-specific assessments of the severe accident risks for the McGuire and Catawba nuclear power plants [1,2] were reviewed to determine applicable types of severe accidents. Both the frequency- and risk-dominant accident sequences were identified and selected for comparative normal LEU versus 40% MOX (core with 40% MOX and 60% LEU assemblies) severe accident simulations. These simulations were performed using the MELCOR severe accident analysis code [3], and generated estimates of radioactive environmental source terms for a set of representative risk-significant accident sequences. This paper summarizes results of the LEU and 40% MOX comparative source term calculations.

II. MELCOR MODEL DESCRIPTION

Catawba Units 1 and 2 and McGuire Units 1 and 2 are each Westinghouse 4-loop PWRs with ice condenser containments. Each of the four plants is similar in design, and a single representative MELCOR model was developed for this study. This section provides a brief description of the MELCOR model used in the source term analyses presented herein. Section II.A describes the basic features of the models for the 4-loop Westinghouse nuclear steam supply system and the ice condenser containment. Section II.B details the basis for the fission product inventories and associated decay heats used for the LEU and the 40% MOX cores. Finally, Section II.C describes the fission product release models used, along with some model comparisons against relevant experimental fission product release data.

II.A. PWR Ice Condenser MELCOR Model

The McGuire and Catawba nuclear power plants both have a 4-loop Westinghouse reactor coolant system (RCS) with an ice condenser containment. A state-of-the-art 4-loop Westinghouse PWR ice condenser MELCOR model has previously been developed [4] based on the Sequoyah nuclear power plant. The designs of the Sequoyah nuclear power plant were compared to the McGuire and Catawba plants. The results of that comparison showed relatively few differences in the key parameters affecting the transients to be performed in this study. Plant-specific modifications were made to the model to accurately represent core power, the refueling storage water tank (FWST), the containment flooding behavior, and the potential for passive flow from the FWST to the reactor during a station blackout accident. The MELCOR RCS and containment nodalization diagrams are shown in Fig. 1 and Fig. 2, respectively.

The MELCOR vessel and RCS nodalization included provisions for in-vessel natural circulation, hot leg counter-current natural circulation, and steam generator natural circulation. New models were implemented to permit two, simultaneously operating fission product release models for a mixed LEU and MOX fuel. A full-scope containment model represented the plant's key containment engineering safety features, including a

Sandia is a multiprogram laboratory operated by Sandia Corporation, a Lockheed Martin Company, for the Department of Energy's National Nuclear Security Administration under contract DE-AC04-94-AL85000

model of the ice chests, which includes ice melting and fission product retention.

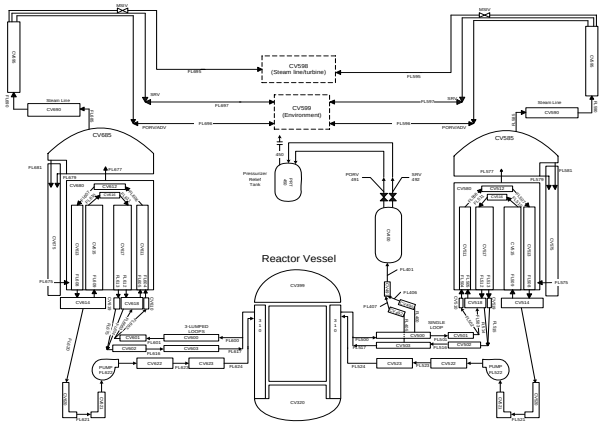

Fig. 1. MELCOR RCS Nodalization Diagram.

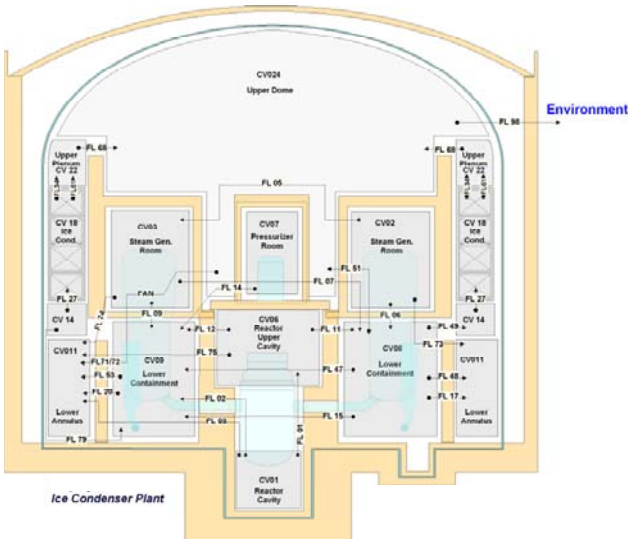

Fig. 2. MELCOR Containment Nodalization Diagram.

II.B. Fission Product Inventories

The Oak Ridge National Laboratory (ORNL) computer code, ORIGEN2.2 [5] was used to determine the elemental composition of irradiated LEU/MOX PWR fuel assemblies and these results were subsequently used to generate inventories for MELCOR radionuclide (RN) class input data. Each of the Catawba and McGuire units are licensed to produce 3411 MW_{th} thermal power. The reactor cores house 193 fuel assemblies of the 17x17 design, with 264 fuel pins per assembly. The WG-Pu MOX fuel assemblies are based on the Framatome/ COGEMA Fuels Advanced Mark BW 17x17 fuel assembly. The ceramic PuO_2 and UO_2 fuel pellets in WG-Pu MOX fuel contain between 2 to 5% fissile plutonium [2]. The isotopic composition vector of the WG Pu MOX fuel is 93.6% 239Pu, 5.9% 240Pu, 0.4% 241Pu, and 0.1% 242Pu, and the UO2 component, has an enrichment of 0.25 wt % 235U. Enrichments used in this analysis were 4.364 weight percent (wt %) 239Pu for the MOX fuel assemblies and 4.236 wt % 235U for the LEU assemblies. Listed in Table 1 are other parameter values used in the ORIGEN2.2 calculation.

Table 1. Operating and Fuel Assembly Data

PARAMETER	VALUE
Reactor design	4-loop Westinghouse PWR
Thermal power	3411 MW(t)
Specific power level	38.7 kW/kg-HM
Fuel cycle duration	495 days [18 months]
Heavy metal per assembly	463.3 kg/assembly
Weight of fuel if UO_2	99,887.0 kg
Cladding weight	25,782.7 kg of Zircaloy 4
FEED ASSEMBLIES FOR 40% MOX CORE	
UO_2 feed assemblies	48
MOX feed assemblies	36
FEED ASSEMBLIES FOR 100% LEU CORE	
UO_2 feed assemblies	84

Mission goals and administrative restrictions were taken into account in determining end of cycle (EOC) values for which to calculate LEU/MOX PWR fuel assembly inventories. One mission goal is to achieve at least one cycle of reactor irradiation on all MOX fuel assemblies while achieving a burnup of at least 20,000 MWd/ MTHM. The specified assembly average MOX fuel burnup limit is 45,000 MWd/MTHM [2]. Thus, in the ORIGEN2.2 model MOX fuel assemblies were irradiated for up to two cycles (average discharge burnup of 38,313 MWd/MTHM). The criterion used for the LEU burnup is the current operational limit of 60,000 MWd/MTU. In the model, LEU fuel assemblies were irradiated for three cycles attaining a maximum discharge burnup of 57,470 MWd/MTHM. Table 2 lists EOC burnup values used in the ORIGEN2.2 runs.

Table 2. Cycle Burnup Used in ORIGEN2.2 Runs

FUEL CYCLE	BURNUP (MWd/MTHM)
1	19,157
2	38,313
3	57,470

A nominal 40% MOX loading pattern for the Catawba and McGuire units is shown in Fig. 3 [6]. There are one hundred ninety-three (193) fuel assemblies in each core. Of these assemblies, one hundred seventeen (117) are LEU and seventy-six (76) are MOX. Table 3 lists the condition of the assemblies (i.e., fresh fuel, once , twice, or three times burned) at the beginning of cycle (BOC) and end of cycle (EOC). Fig. 4 represents the configuration for a typical LEU loading pattern [6].

Table 4 lists the condition for those assemblies. Since accident analyses typically assume higher fission-product build-up EOC conditions, the MELCOR MOX and LEU core descriptions were assembled based on the EOC assembly conditions of Table 3 and Table 4, respectively.

1					L-2	M-1	L-2	M-1	L-2	M-1	L-2				
2			L-2	L-1	M-0	L-0	M-0	L-0	M-0	L-0	M-0	L-1	L-2		
3		L-2	M-0	M-0	L-0	M-1	M-1	L-0	M-1	M-1	L-0	M-0	M-0	L-2	
4		L-1	M-0	L-1	L-1	M-1	L-0	L-1	L-0	M-1	L-1	L-1	M-0	L-1	
5	L-2	M-0	L-0	L-1	M-1	M-0	L-1	L-0	L-1	M-0	M-1	L-1	L-0	M-0	L-2
6	M-1	L-0	M-1	M-1	M-0	L-1	L-0	L-1	L-0	L-1	M-0	M-1	M-1	L-0	M-1
7	L-2	M-0	M-1	L-0	L-1	L-0	L-1	L-0	L-1	L-0	L-1	L-0	M-1	M-0	L-2
8	M-1	L-0	L-0	L-1	L-0	L-1	L-0	L-2	L-0	L-1	L-0	L-1	L-0	L-0	M-1
9	L-2	M-0	M-1	L-0	L-1	L-0	L-1	L-0	L-1	L-0	L-1	L-0	M-1	M-0	L-2
10	M-1	L-0	M-1	M-1	M-0	L-1	L-0	L-1	L-0	L-1	M-0	M-1	M-1	L-0	M-1
11	L-2	M-0	L-0	L-1	M-1	M-0	L-1	L-0	L-1	M-0	M-1	L-1	L-0	M-0	L-2
12		L-1	M-0	L-1	L-1	M-1	L-0	L-1	L-0	M-1	L-1	L-1	M-0	L-1	
13		L-2	M-0	M-0	L-0	M-1	M-1	L-0	M-1	M-1	L-0	M-0	M-0	L-2	
14			L-2	L-1	M-0	L-0	M-0	L-0	M-0	L-0	M-0	L-1	L-2		
15					L-2	M-1	L-2	M-1	L-2	M-1	L-2				
	O	N	M	L	K	J	I	H	G	F	E	D	C	B	A

Fig. 3. Projected Loading Pattern for 40% MOX Core.

Table 3. Assemblies in 40% MOX Core

PREVIOUS CYCLES IN CORE	BOC		EOC	
	LEU	MOX	LEU	MOX
Zero (Feed)	48	36	-	-
One	44	40	48	36
Two	25	-	44	40
Three	-	-	25	-

1					L-2	L-1	L-2	L-1	L-2	L-1	L-2				
2			L-2	L-1	L-0	L-1	L-0	L-1	L-0	L-1	L-0	L-1	L-2		
3		L-2	L-1	L-0	L-1	L-0	L-1	L-0	L-1	L-0	L-1	L-0	L-1	L-2	
4		L-1	L-0	L-1	L-1	L-1	L-0	L-2	L-0	L-1	L-1	L-1	L-0	L-1	
5	L-2	L-0	L-1	L-1	L-1	L-0	L-1	L-0	L-1	L-0	L-1	L-1	L-1	L-0	L-2
6	L-0	L-1	L-0	L-1	L-0	L-2	L-0	L-2	L-0	L-2	L-0	L-1	L-0	L-1	L-0
7	L-2	L-0	L-1	L-0	L-1	L-0	L-1	L-0	L-1	L-0	L-1	L-0	L-1	L-0	L-2
8	L-0	L-1	L-0	L-2	L-0	L-2	L-0	L-2	L-0	L-2	L-0	L-2	L-0	L-1	L-0
9	L-2	L-0	L-1	L-0	L-1	L-0	L-1	L-0	L-1	L-0	L-1	L-0	L-1	L-0	L-2
10	L-0	L-1	L-0	L-1	L-0	L-2	L-0	L-2	L-0	L-2	L-0	L-1	L-0	L-1	L-0
11	L-2	L-0	L-1	L-1	L-1	L-0	L-1	L-0	L-1	L-0	L-1	L-1	L-1	L-0	L-2
12		L-1	L-0	L-1	L-1	L-1	L-0	L-2	L-0	L-1	L-1	L-1	L-0	L-1	
13		L-2	L-1	L-0	L-1	L-0	L-1	L-0	L-1	L-0	L-1	L-0	L-1	L-2	
14			L-2	L-1	L-0	L-1	L-0	L-1	L-0	L-1	L-0	L-1	L-2		
15					L-2	L-1	L-2	L-1	L-2	L-1	L-2				
	O	N	M	L	K	J	I	H	G	F	E	D	C	B	A

Fig. 4. Typical Loading Pattern for LEU Core.

Table 4. Assemblies in LEU Core

CYCLES IN CORE	BOC	EOC
Zero (Feed)	80	-
Once	76	80
Twice	37	76
Three times	-	37

The MOX and LEU element masses and specific powers formed from the ORIGEN results were input to MELCOR along with a specification for combining the individual elements into radionuclide classes. The combination of elements into classes was performed in accordance with MELCOR default scheme per Table 5. Representative elements for each class are identified in **bold**. Resulting MELCOR fission product mass inventories for an LEU core and a 40% MOX core (including contributions from LEU and MOX assemblies) are listed in Table 6.

Table 5. Radionuclide Class Constitutive Elements

CLASS NAME	CONSTITUTIVE ELEMENTS
Noble Gases	Kr, **Xe**
Alkali Metals	**Cs**, Rb
Alkaline Earths	**Ba**, Sr
Halogens	Br, **I**
Chalcogens	Se, **Te**
Platinoids	Pd, Rh, **Ru**
Transition Metals	**Mo**, Nb, Tc
Tetravalents	**Ce**, Np, Pu, Zr
Trivalents	Cm, Eu, **La**, Nd, Pm, Pr, Sm, Y
Uranium	**U**
More Volatile Metals	As, **Cd**, Sb
Less Volatile Metals	Ag, Ge, In, **Sn**
Boron	**B**

Table 6. Radionuclide Class Masses At Shutdown (kg)

CLASS	LEU CORE	40% MOX CORE		
		LEU	MOX	TOTAL
Xe	517.8	318.7	169.4	488.1
Cs	291.0	178.7	100.9	279.6
Ba	220.0	135.2	54.92	190.1
I	23.46	14.44	11.37	25.81
Te	48.65	29.98	20.50	50.48
Ru	359.2	222.1	187.4	409.5
Mo	372.8	229.2	120.8	350.0
Ce	1489.	913.4	1300.	2213.
La	699.6	430.5	210.5	641.0
U	85,020	51,510	32,880	84,390
Cd	14.91	9.256	8.470	17.73
Sn	14.84	9.166	9.360	18.53
B	0.	0.	0.	0.

As expected, the EOC inventory for the MELCOR "Ce" class, which includes all Pu isotopes as constituents, is 49% larger for the 40% MOX core than the LEU core. Table 7 shows the EOC Pu inventory, both in terms of total fission product mass and in terms of radioactivity.

Fig. 5 shows the time history of fission product decay power for the LEU and MOX cores. For comparison purpose, the standard ANS decay power curve is also shown.

Table 7. EOC Pu Fission Product Comparison

EOC Pu VALUES	LEU CORE	40% MOX CORE	% Increase
Mass (kg)	846	1657	94
Activity (Ci)	21.4E+06	40.1E+06	87

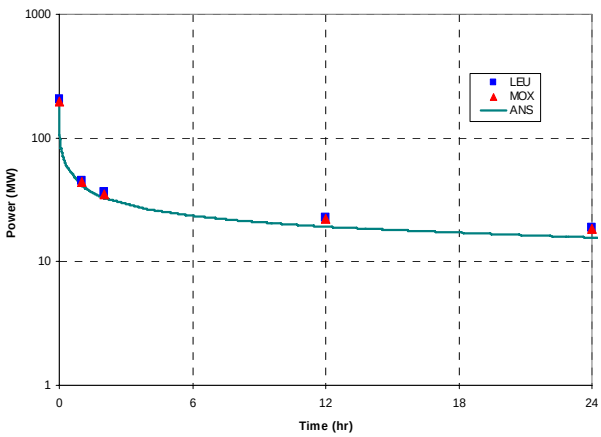

Fig. 5. Fission Product Decay Power.

II.C. Fission Product Release Model

Review of available experimental data suggests that differences exist in the fission product release rates for some fission product groups under certain temperature conditions. The VERCORS RT-2 test [7] was performed using MOX fuel from the Gravelines nuclear power plant in France having a burnup of approximately 47.3 MWd/ tonne. The objective of the VERCORS tests was to provide fission product release measurements for use in developing and validating models predicting such release under severe accident or off-normal conditions. The RT-2 test was analogous to the RT-1 test, which was performed using normal LEU fuel. Both tests were performed under similar conditions with a mixture of steam and hydrogen (0.5:25 mg/s of H2:H20) during fission product release up to temperatures nearing 2500K. Neither test RT-1 or RT-2 involved any re-irradiation of the test fuel samples prior to testing and, because of this, no data was obtained on the release of iodine or other short lived fission products. The test measurements focused on release of krypton, cesium, ruthenium, cerium, and europium, the latter three of which are generally considered to be of low volatility in comparison to cesium and iodine. The principal measurement in test RT-2 was for the time temperature release of cesium, the results of which are shown in Fig. 6. (A second MOX fission product release test was performed in the VERCORS program, test RT-7 [8]. This test was performed with release under pure reducing conditions. Since fission product release is expected to take place with both steam and hydrogen present, the RT-7 data are not considered representative of in vessel release conditions overall, and for this reason are not considered this study.) Total releases for other isotopes measured in tests RT-1 (LEU) and RT-2 (MOX) are summarized in [8].

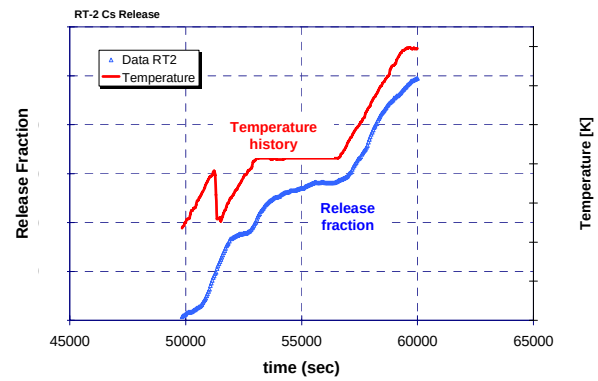

Fig. 6. RT-2 Cs Release as a Function of Temperature.[1]

The Booth diffusion model is one model available in MELCOR for calculating the release of fission products from overheating fuel, and is selected for this study because of its more mechanistic nature in comparison to the CORSOR fractional release rate models. In this treatment, the release of Cs is modeled to match the kinetics of the measured release for Cs, and other fission product releases are simply scaled to the Cs release to match that observed experimentally. The Booth release model is described briefly below.

In the Booth model, as implemented in MELCOR, the release of Cs from the fuel is treated as a diffusion process where Cs migrates through the fuel matrix to the surface of a fuel grain. From there, a mass transport limitation based on specie vapor pressure is considered prior to release to the local atmosphere. The effective diffusion coefficient for cesium in the fuel grain is calculated as shown in Eq. 1, where R is the universal gas constant, T is the temperature, Q is an activation energy, and the pre exponential factor D_0 is a function of the fuel burn up.

$$D = D_0 \exp(-Q/RT). \qquad (1)$$

The cesium release fraction at time t is calculated from an approximate solution of the diffusion equation for fuel grains of spherical geometry [9], as shown in Eqs. 2 and 3,

$$f = 6\sqrt{\frac{D't}{\pi}} - 3D't \;\; for \; D't < 1/\pi^2 \qquad (2)$$

[1] The units are omitted from the graph because the data are considered proprietary.

$$f = 1 - \frac{6}{\pi^2}\exp\left(-\pi^2 D't\right) \; for \; D't \geq 1/\pi^2 \qquad (3)$$

where

$D't$ = Dt/a^2 (dimensionless), and
a = equivalent sphere radius for the fuel grain.

The parameters of the diffusion coefficient, D_o and Q, may be determined from experimental data by a fitting process described by Lorenz and Osborne [10]. In this process, Eq. 4 and 5 are inverted to solve for the product Dt/a^2, as indicated below, where f is the release fraction.

$$\frac{Dt}{a^2} = \frac{2}{\pi} - \frac{f}{3} - 2\sqrt{\frac{1}{\pi^2} - \frac{f}{3\pi}} \; for \; f < 0.85 \qquad (4)$$

$$\frac{Dt}{a^2} = \frac{1}{\pi^2}\ln\left[\frac{\pi^2(1-f)}{6}\right] \; for \; f \geq 0.85 \qquad (5)$$

These forms may be used to plot the apparent instantaneous measured diffusion coefficient as a function of the measured temperature as shown in Fig. 7. Also shown in this figure are two fits of the diffusion coefficient (Eq. 1), one for MOX determined by inspection for the RT-2 data shown in red, and another shown in blue found to represent well Cs release from LEU fuel. As can be seen, there are significant differences in the apparent Cs diffusion coefficient for MOX fuel in comparison to release from LEU fuel. The parameters used to represent Cs diffusion release from MOX and LEU fuel are summarized in Table 8.

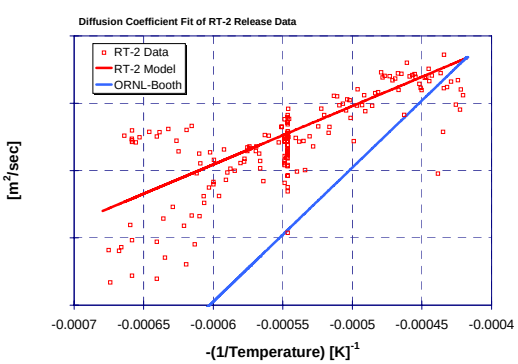

Fig. 7. RT-2 Cesium Release Data as a Function of Time Using Inverted Booth Solution.[2]

The Booth parameters for Cs release from MOX fuel determined from the RT-2 data are used in a MELCOR model of the RT-2 test to assess the predicted release against that observed experimentally. The results of the

Table 8. Diffusion Coefficient Parameters

	Do [m^2/s]	Q [J/kg-mole]
LEU Fuel (ORNL-Booth)	$1x10^{-6}$	$3.814x10^5$
MOX Fuel (MOX-Booth)	$2x10^{-11}$	$1.664x10^5$
Grain radius	6μm	6μm

MELCOR release prediction for Cs in test RT-2 are shown in Fig. 8. The kinetics of Cs release are well predicted by the MOX Booth diffusion parameters, and the low temperature release rate compared to that of LEU fuel (ORNL Booth) is greater for the same assumed temperature history. Significant release of Cs from MOX fuel is observed fuel to begin at lower temperatures than for LEU fuel. However, for temperatures indicative of severe accident fuel melt and relocation, release rates are similar. MELCOR predictions were also compared to data from RT-2 measurements (or FPT 1 measurements for the release classes where RT-2 measurements were not available). All comparisons showed reasonable agreement. The revised Booth release model for MOX fuels was applied to the MOX assemblies in all MELCOR calculations that simulated the 40% MOX core.

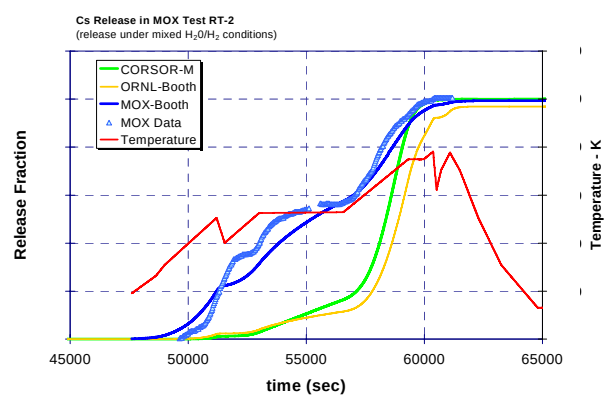

Fig. 8. Comparison of the MELCOR-Predicted Release of Cesium-Class for VERCORS Test RT-2 to the Experimental Measurement of Cs-137.[3]

III. ACCIDENT SEQUENCES CONSIDERED

To examine the impact of a 40% MOX core during a postulated severe accident, a set of risk-dominant MELCOR calculations was specified. The calculations

[2] Also shown are fits for D(T) determined from the MOX data and the form recommended for LEU use (modified ORNL Booth coefficients). Again, proprietary data values are removed from dependent axis.

[3] Also shown are MELCOR-predicted releases using the MELCOR default Cs release model (CORSOR-M) and the presently recommended ORNL-Booth release model for LEU fuel.

parametrically include fission product releases with and without MOX fuel for each scenario. Four accident initiators were selected along with two containment end states. The accident initiators considered included station blackout (SBO), small-break loss of coolant accident (SLOCA) with failure to realign the emergency core cooling system (ECCS), large-break loss of coolant accident (LLOCA) with failure of the ECCS, and SBO with induced steam generator tube rupture (ISGTR). The containment end states considered were early failure (failure due to lower head failure at high pressure) and late failure due to slow pressurization from core-concrete interaction (all others).

Considering the various accident initiators, SBOs account for 43% of the total core damage frequency (CDF) in Revision 2b of the Catawba PRA [2]. LOCAs account for 30% of the total. SLOCAs are larger contributors than LLOCAs, and failure to accomplish switchover of high pressure injection to recirculation mode is the dominant cause of core damage in a SLOCA.

The contribution to total CDF of steam generator tube rupture (SGTR) is small but thought to be under-estimated in the current Catawba PRA [2]. In the McGuire PRA [1], bypass failure of containment has a relatively significant frequency and is largely dominated by ISGTR. Loss of offsite power initiators are important contributors to the ISGTR sequences. Therefore, ISGTR calculations were included in the MELCOR calculation set. The hot gasses that are generated in the core and re-circulated through the steam generator tubes are responsible for the induced steam generator tube failures.

IV. SOURCE TERM RESULTS

MELCOR simulations were performed for each of the accident sequences described above for an LEU core, and then again for a 40% MOX core. Accident progression signatures qualitatively followed those traditionally observed for these sequences, which are commonly evaluated as part of PWR risk assessments. Selected results are presented here for the frequency-dominant accident, the SBO with late containment failure. A listing of key events observed in the MELCOR simulation is provided in Table 9. Note that accident progression timing is not significantly affected by whether the accident involves an LEU or a 40% MOX core. Differences observed are well within uncertainties typically associated with severe accident analysis.

Times corresponding to risk-significant release phases are identified in Table 10. Selected accident signatures are shown in Fig. 9 through Fig. 13.

Table 9. Key Events for SBO, Late Containment Failure

Event	LEU Core (hr)	40% MOX Core (hr)
Loss of ac power	0.0	0.0
Pump seals leak at 21 GPM	0.0	0.0
Loss of dc power	3.0	3.0
SG secondary dry	5.9	5.9
Rx water level below TAF	6.5	6.6
Start of fuel cladding failures	8.0	8.1
Hot leg nozzle creep failure	9.7	9.9
Containment design pressure	9.7	9.8
Accumulator injection starts	9.7	9.9
First H_2 burn in containment	9.7	9.9
Accumulators empty	9.7	9.9
Start of core plate failures	11.3	11.6
Debris relocation to lower head	14.3	13.6
Vessel failure	17.9	16.7
Containment failure	70.2	68.7

Table 10. Timing of Risk-Significant Fission Product Release Phases

ONSET OF RELEASE AND RELEASE DURATIONS	LEU Core (hr)	40% MOX Core (hr)
Onset of release of radionuclides	6.5	6.6
Coolant activity release duration	1.5	1.5
Gap release duration	0.5	0.7
In-vessel release duration	9.4	7.9

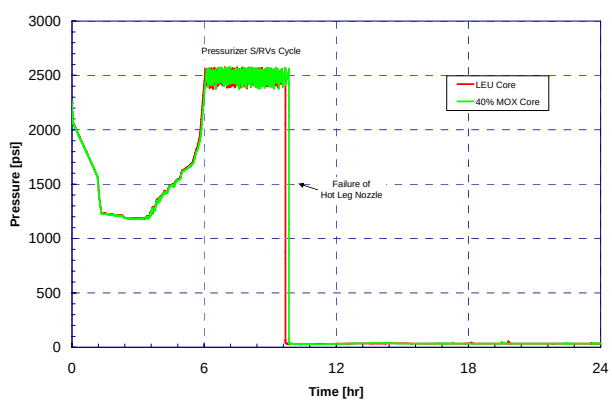

Fig. 9. SBO, RCS Pressure

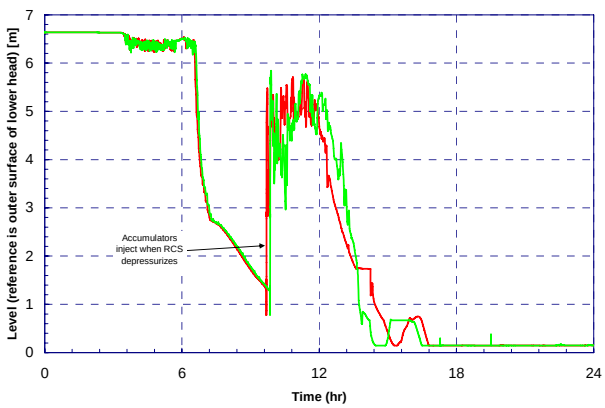

Fig. 10. SBO, Reactor Vessel Coolant Level

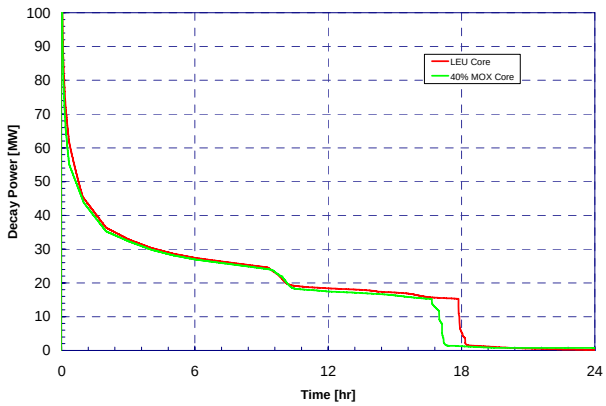

Fig. 11. SBO, Decay Power of Fission Products Remaining in Fuel.

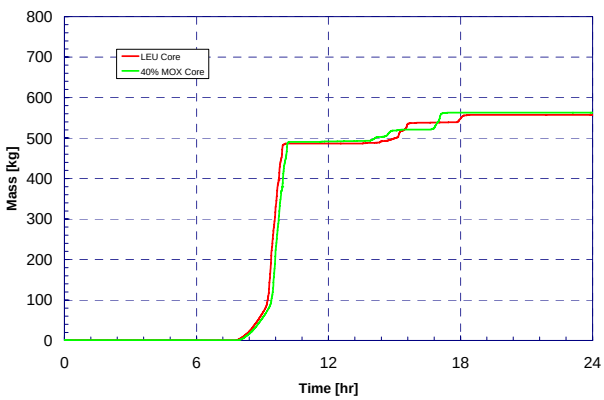

Fig. 12. SBO, Hydrogen Produced In-vessel.

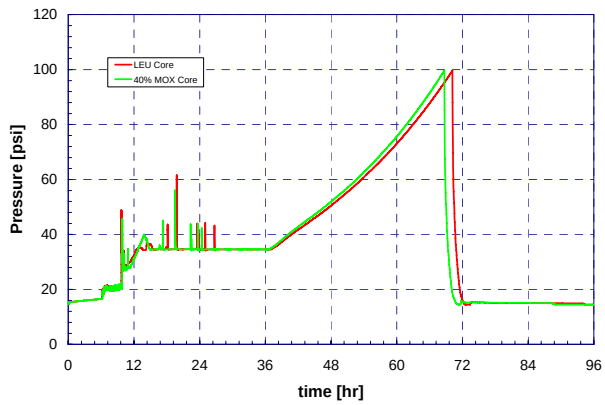

Fig. 13. SBO, Containment Pressure.

To compare results from calculations with an LEU core to results from calculations with a 40% MOX core, the release fractions from the RCS (i.e., to containment) are shown in Table 11 for the risk-significant early release phase. Differences observed between the two core types are well within normal uncertainties for source term calculations.

Table 11. SBO, Release Fractions to Containment for Early Phase

MELCOR GROUP	LEU CORE	40% MOX CORE
Xe	0.905	0.918
Cs	0.643	0.646
Ba	0.0020	0.0019
I	0.750	0.769
Te	0.653	0.680
Ru	0.0097	0.0071
Mo	0.461	0.420
Ce	$2x10^{-7}$	$1x10^{-7}$
La	$2x10^{-7}$	$2x10^{-7}$

While examination of release timing, qualitative accident progression signatures, and fission product release fractions (from the RCS) did not show substantial differences between accident simulations for an LEU core and for a 40% MOX core, it is instructive to compare releases of fission product masses to the environment when attempting to draw conclusions about risk. One might hypothesize that due to increased fission product inventories for some radionuclide classes, environmental releases would be increased for the 40% MOX Core. Fig. 14 through Fig. 17 show some of these comparisons for consequence-significant fission products for the SBO sequences analyzed. On the figures are both the SBO base case response described previously as well as an early containment failure sensitivity study, which led to large environmental releases following vessel failure. The early containment failure results are characterized by

a large, early release following simultaneous vessel and containment failure. The late containment failure cases have early releases due to calculated leakage and a large, late release at the time of late containment failure. In both containment failure scenarios, the environmental releases for the LEU core calculations and the 40% MOX core calculations are similar. Note that this is even true for the Ce class, which had the largest increase in the EOC inventory.

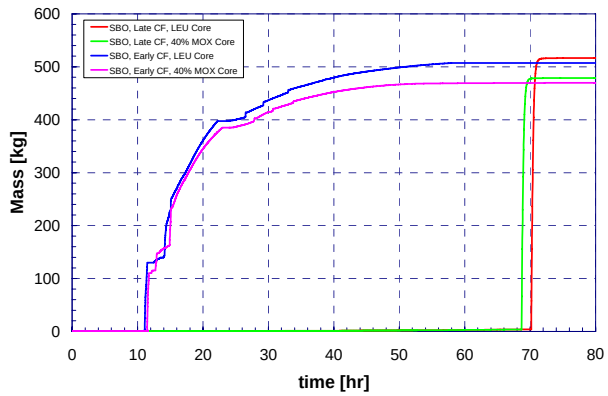

Fig. 14. Xe Group - SBO Release to Environment

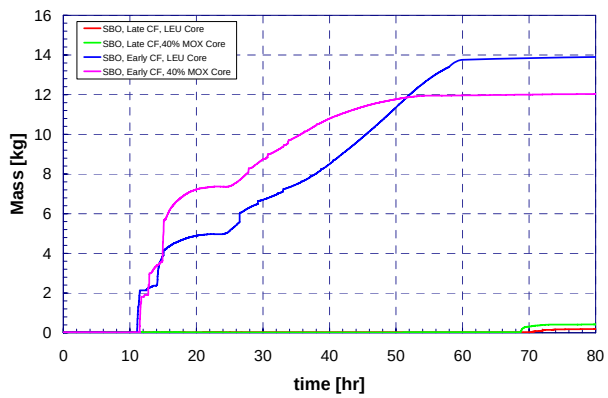

Fig. 15. Cs Group - SBO Release to Environment

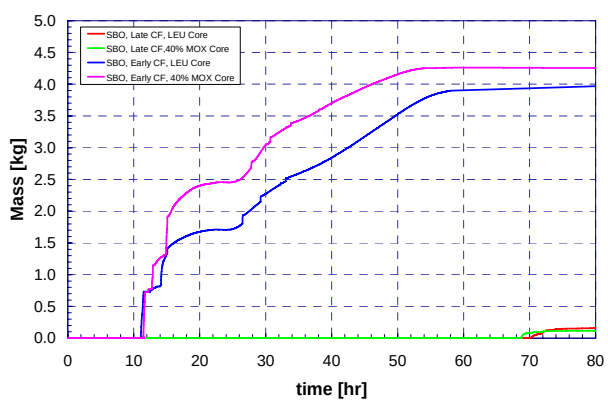

Fig. 16. I Group - SBO Release to Environment

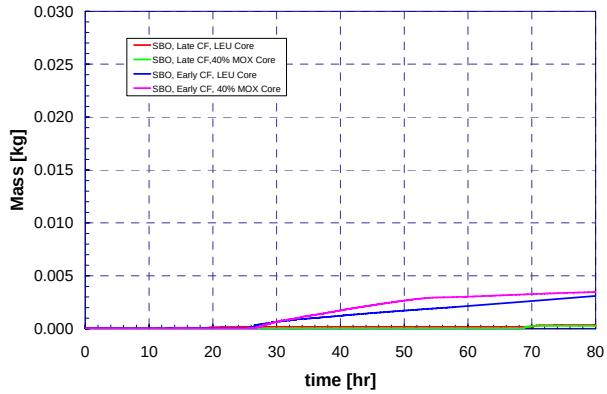

Fig. 17. Ce Group - SBO Release to Environment

V. SUMMARY AND CONCLUSIONS

For each of the accident categories identified as frequency- or risk-dominant, separate MELCOR calculations were performed for LEU and 40% MOX cores. In general, fission product release from the fuel and to the environment for LEU and 40% MOX cases were similar. This was initially unexpected, because (a) it was thought that fission product inventories for the 40% MOX core would be noticeably higher than the LEU Core and (b) experimental data for fission product releases from MOX fuel suggest a lower temperature onset of significant releases than LEU. However, ORIGEN calculations were performed to estimate end-of-cycle fission product inventories for a typical LEU and a proposed 40% MOX cycle. Administrative limits on MOX assembly loading and burnup limited the calculated fission product inventories for the MOX assemblies; thus the increase for some radioactive elements in the 40% MOX core was smaller than expected, and inventories were smaller for some elements significant to health consequences (e.g., Cs). In addition, the MELCOR calculations show that under expected severe accident conditions, volatile fission product releases occur at very high release rates owing to high fuel temperatures, regardless of the fuel type. Hence, differences noted in experimental results at lower temperatures do not produce appreciable differences in net volatile releases under severe accident conditions.

For most accident scenarios and fission product types, LEU release rates were slightly higher than 40% MOX cases for two reasons. First, the LEU core had a higher average and maximum assembly burnup, increasing the core-wide fission product inventory. Consequently, for the same fission product release fraction, LEU mass released is higher. Second, higher LEU burnup fuel had a higher decay power. Therefore, the accident progressed somewhat more quickly with somewhat higher fuel temperatures (i.e., leads to higher fission product releases). Having said this, observed

differences in release quantities are considered to be less than variations due to more global accident progression uncertainties.

In some specific cases and fission product classes, 40% MOX release rates were higher than LEU release rates. These differences can be traced to two causes. For some fission products, the 40% MOX inventory was higher than the LEU inventory (e.g, the "tetravalent" fission product class, including Pu). Second, global phenomenological uncertainties caused variations in calculated accident progression contributing to different localized release rates for some sequences. In particular, some late phase uncertainties can cause significant changes in the accident response and late fission product releases. The series of calculations represent point estimates to the calculated response. However, previous studies which systematically evaluated severe accident uncertainties [e.g., Ref. 4] show variations in LEU response that bounds the differences noted in the present report. Hence, no significant fission product release differences were noted in the LEU and 40% MOX severe accident response for the wide range of risk-significant transients considered.

Conclusions drawn here stop short of evaluating whether there is an increased risk in operation of the McGuire and Catawba plants with a 40% MOX core. Comparison of source terms calculated for LEU cores against 40% MOX cores indicate little difference, in terms of released mass for any given MELCOR release class. However, a detailed evaluation of the public health and environmental consequences has not been performed. Differences in specific-activities, as well as other issues, would need to be considered in a comprehensive risk evaluation.

ACKNOWLEDGMENTS

This work was supported by the U.S. NRC, Office of Nuclear Regulatory Research (RES).

REFERENCES

1. Duke Energy Corporation, McGuire Nuclear Station, IPE Submittal Report, 1992.
2. Duke Energy Corporation, Catawba Nuclear Station, IPE Submittal Report, 1992.
3. R.O. GAUNTT, *et al.*, "MELCOR Computer Code Manuals, Version 1.8.5," NUREG/CR 6119, Rev. 2, October 2000.
4. R.O. GAUNTT and K.C. WAGNER, "An Uncertainty Analysis of the Hydrogen Source Term for a Station Blackout Accident in Sequoyah Using MELCOR 1.8.5," Sandia National Laboratories Letter Report to U.S. NRC, October 2002.
5. S.B. LUDWIG, and J.P. RENIER, "Standard and Extended Burnup PWR and BWR Reactor Models for the ORIGEN2 Computer Code," ORNL/TM 11018 (December 1989), CCC 0371/17.
6. "Nuclear Design Methodology Using CASMO 4/SIMULATE 3 MOX," Duke Power Corporation, DPC NE 1005P, Revision 0, 2001.
7. F. CECCALDI, *et al.*, "Rapport de Synthese de l'essai VERCORS RT2," CEA Note Technique DEC/S3C/01 013, March 8, 2001.
8. Y. PONTILLON, *et al.*, "Rapport de Synthese de l'essai VERCORS RT7," CEA Note Technique DEC/S3C/01 002, July 23, 2001.
9. T. NAKAMURA, and R.A. LORENZ, "A Study of Cesium and Krypton Releases Observed in HI and VI Tests Using a Booth Diffusion Model," Oak Ridge National Laboratory Research Paper May 1987.
10. R.A. LORENZ, and M.F. OSBORNE, "A Summary of ORNL Fission Product Release Tests with Recommended Release Rates and Diffusion Coefficients," NUREG/CR 6261, 1995.